Appl. Phys. B (2016) 122:241
DOI 10.1007/s00340-016-6519-4

Applied Physics B
Lasers and Optics

Two side liquid-cooled and passively Q-switched disk oscillator with nanosheets in flowing CCl_4

Rongzhi Nie[1,2] · Jiangbo She[1] · Dongdong Li[4] · Fuli Li[2] · Bo Peng[1,3]

Received: 6 May 2016 / Accepted: 24 August 2016 / Published online: 30 August 2016

Abstract A passively Q-switched and two side liquid-cooled Nd:YAG disk oscillator is demonstrated, which is operated at a pump pulse width of 300 μs and a pump repetition rate of 10 Hz. The coolant flows over the two large surfaces of the disk and will be passed through by laser beam, so it can also serve as a saturable absorber. For the unmodulated laser, the pure CCl_4 was employed as coolant and a plane output mirror of 15 % transmission was employed. The maximum output energy of 795 mJ is realized corresponding to the optical–optical efficiency of 27.4 % and the slope efficiency of 30 %; for the graphene Q-switched laser, the CCl_4 with graphene nanosheets was employed as coolant and a plane output mirror of 40 % transmission was employed. The maximum output energy of 376 mJ is realized corresponding to the optical–optical efficiency of 13 % and the slope efficiency of 18 %. The maximum average Q-switching repetition rate is 385 kHz, and the minimum average pulse width is 116 ns; for the MoS_2 Q-switched laser, the CCl_4 with MoS_2 nanosheets was employed as coolant and a plane output mirror of 30 % transmission was employed. The maximum output energy of 486 mJ is realized corresponding to the optical–optical efficiency of 17 % and the slope efficiency of 22 %.The maximum average Q-switching repetition rate is 470 kHz, and the minimum average pulse width is 137 ns.

✉ Jiangbo She
shejb@opt.ac.cn

✉ Bo Peng
bpeng@opt.ac.cn

[1] State Key Laboratory of Transient Optics and Photonics, Xi'an Institute of Optics and Precision Mechanics, Chinese Academy of Science (CAS), Xi'an 710119, China

[2] School of Science, Xi'an Jiaotong University, Xi'an 710119, China

[3] Key Laboratory for Organic Electronics and Information Displays, Institute of Advanced Materials (IAM), Nanjing University of Posts and Telecommunications, Nanjing 210046, Jiangsu, China

[4] School of Electronic Engineering, Xi'an University of Post and Telecommunications, Xi'an 710121, China

1 Introduction

Q switching is an important and major technique for generating short laser pulses in μs and ns time durations. Passively Q-switched solid-state laser (SSL) with high peak power and short pulse width has attracted a great deal of attention for applications in material processing, laser-induced plasma spectroscopy (LIPS), laser ranging, laser communication, remote sensing, and medicine. However, operation of a SSL produces a significant amount of waste heat. Thermally induced effects, such as thermal lens, thermal birefringence, and thermal stress [1], limit the output energy and beam quality of SSL. Worst of all, extremely high thermal intensity will exceed damage thresholds of both solid laser gain materials and passively Q-switched materials. Therefore, researchers still have strong motivations and are making every effort to seek new cooling method and passively Q-switched materials with high damage threshold.

Extensive investigations suggest that the maximum achievable heat transfer rate of gas flow cooling is about 5 W/cm^2 [2]. As a comparison, liquid flow cooling can easily handle heat fluxes around 100 W/cm^2 [3], which is more efficient than gas flow cooling and well suited for high output SSL. Combining the advantages of disk laser and liquid forced convection heat transfer, the two-sided liquid cooling disk laser configuration was proposed in recent years

[4–8]. In this configuration, the two large faces of disk-type gain medium are both cooled by flowing liquid, which will enhance cooling efficiency dramatically. Unlike the two-sided cooling slab laser, this laser configuration allows laser passing through the large aperture and outputs a symmetric beam. At the same time, arrangement of laser gain medium is more flexible and bending of the disk due to different cooling rates of its front and back side is avoided. In our previous work [9], this laser configuration and its profiles were demonstrated. Based on the two-sided liquid cooling configuration, we developed a suitable passively Q-switching technology with flowing liquid SAs (saturable absorbers).

By dispersing the nanosheets SAs in flowing CCl_4 (carbon tetrachloride), the heat of SAs can be dissipated rapidly so that the nanosheet can withstand high optical power. Additionally, nanosheets (SAs) flow with CCl_4 circularly to avoid performance degradation due to excess heat. The flowing SAs are based on 2D (two-dimensional) materials represented by graphene [10], graphene oxide [11, 12], and TMDCs (transition metal dichalcogenides) [13–15] due to their broadband absorption, ultrafast carrier dynamics, and planar characteristics.

In this paper, we demonstrate a new kind of passively Q-switched thin-disk laser by dispersing the graphene and MoS_2 nanosheets into the flowing coolant. With this method, the flowing liquid cannot only help a quick transfer of the generated heat but also serve as the SAs for the passively Q-switched operation.

2 Preparation of the saturable absorber

In this work, nanosheets (serve as SAs) were dispersed in flowing CCl_4 to serve as flowing saturable absorber and coolant. For comparison, monolayer graphene or MoS_2 sheets were dispersed in CCl_4 separately. Monolayer structure was used for the broadband saturable absorption characteristics under the help of the Pauli blocking effect [15, 16]. The purity of graphene is more than 97 %, the thickness of the sheet is 0.33–0.39 nm, and the diameter of the sheet is 100–300 nm. The single layer ratio of MoS_2 nanosheets is more than 95 %, the thickness of the sheet is ~ 1 nm, and the diameter of the sheet is 20–500 nm. The diameter was not optimal in this experiment. For one thing, the 2D nanomaterial has a broad size distribution and it is difficult to separate the nanosheets with different size, so it is almost impossible to make a comparison between different sizes. For another, the range of size cannot be controlled; the aim of providing the diameter is just to describe these nanosheets, not to choose this diameter on purpose. The purity is not optimal, we think the impurities will decrease the efficiency of lasers; unfortunately, it is almost impossible to prepare pure graphene or MoS_2 nanosheets.

One millimole of graphene or MoS_2 nanosheets was poured into 200 ml CCl_4, respectively. After the ultrasonic process of 30 min, the dispersion was centrifuged for 20 min at 10,000 r/min to induce sedimentation of large clusters. The upper portion of the centrifuged solution was decanted to serve as the coolant and the saturable absorber. Using this method, we finally spent 15 mmol nanosheets and prepared 2400 mL suspension liquid. The performance of 2D material depends on the number of layers [17]. Once the monolayer nanosheets agglomerate in the coolant, the performance of monolayer will be influenced. Unfortunately, the monolayer nanosheet is easy to agglomerate due to the high specific surface area. Only the upper portion of the centrifuged solution was utilized as the coolant, for it is considered to have the best dispersity. The experience shows that these SAs can be used for Q-switching operation over 1 month.

The transmission spectra of different nanosheets in CCl_4 were measured by a V-570 spectrophotometer (Jasco, Japan) scanning from 900 to 1900 nm. The sample was injected in a quartz cuvette with an absorption length of 2 cm. In order to exclude the absorption of CCl_4 and the Fresnel reflectance loss, a transmission spectrum of a same quartz cuvette filled with the pure CCl_4 was measured as a reference. Then, the real transmission spectra of two kinds of nanosheets dispersion are shown in Fig. 1. The coefficient of losses (absorption coefficient plus scattering coefficient) is calculated according to Beer–Lambert law: $T = 1-\exp(\alpha l)$. T is the transmission, α is the coefficient of losses, l is the absorption length. Taking the transmission at 1064 nm (98.8 % for graphene and 97.5 for MoS_2) and the absorption length (2 cm) into the formula, the calculated α is -0.006 cm^{-1} (graphene) and -0.012 cm^{-1} (MoS_2).

CCl_4 is used as the cooling liquid for several reasons. Firstly, CCl_4 is a low-cost liquid and has a low freezing point of −22.92 °C, so this kind of laser configuration is not easy to freeze in cold weather. Secondly, CCl_4 is

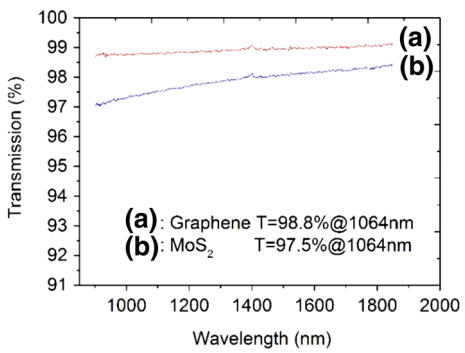

Fig. 1 Linear transmission spectra of different nanosheets in CCl_4 with an absorption length of 2 cm

Table 1 Key heat-related characteristics

	Volume heat capacity (J/m^3 K)	Heat conductivity (W/m K)
CCl_4	1.38×10^6	0.106
Air	1.33×10^3	0.023

optical transparent. At room temperature, (a) CCl_4 has the absorption coefficient of -0.01 cm^{-1} at 808 nm, which is 50 % lower than the case of H_2O (absorption coefficient of -0.02 cm^{-1} @808 nm). (b) CCl_4 has the absorption coefficient of -0.005 cm^{-1} at 1064 nm, which is much lower than the case of H_2O (absorption coefficient of -0.14 cm^{-1} @1064 nm). Thirdly, CCl_4 has a high-volume heat capacity of 1.38×10^6 J/m^3 K, this number is one thousand times as that of air. The heat conductivity is near five times as that of air. The key heat-related characteristics are listed in Table 1.

3 Experiment setup

The experimental setup of two side liquid-cooled disk oscillator and its circulatory system is illustrated in Fig. 2. Two Nd:YAG disks orienting at Brewster's angle are fixed in a chamber. The temperature of flowing coolant is decreased to 10 °C by a refrigerator, and the coolant passes through the chamber from the inlets to the outlets. As shown in Fig. 2b, the coolant passes through two Nd:YAG disks in the opposite direction, so the liquid temperature gradient caused by flowing direction can be compensate. The inlet velocity is 1 m/s. The coolant flows over the two large surfaces of the disk and takes away the deposited heat in the way of forced convection cooling [18]. In the unmodulated operation, the coolant is pure liquid CCl_4. In the passively Q-Switched operation, the coolant is liquid CCl_4 with nanosheets dispersing in it. The internal length of the camber is 6.5 cm. For the graphene, the absorption coefficient plus scattering coefficient is -0.006 cm^{-1} at 1064 nm, corresponding to an absorption and scattering loss of 3.8 % for an absorption length of 6.5 cm. For the MoS_2, the absorption coefficient plus scatting coefficient is -0.012 cm^{-1} at 1064 nm, corresponding to an absorption and scattering loss of 7.5 % for an absorption length of 6.5 cm.

Two pieces of 1.1-at.%-doped Nd:YAG crystal disks are used as laser gain medium. The disk has a dimension of $20 \times 20 \times 2$ (mm). Each disk is face pumped from a single side by a laser diode array (LDA). The pump light is focused and collimated to generate a beam with a cross section of about 10×12 mm. The pump light incidences to the Nd:YAG disk and generates a spot of about 10×16 mm. Finally, these lasers have a laser output spot

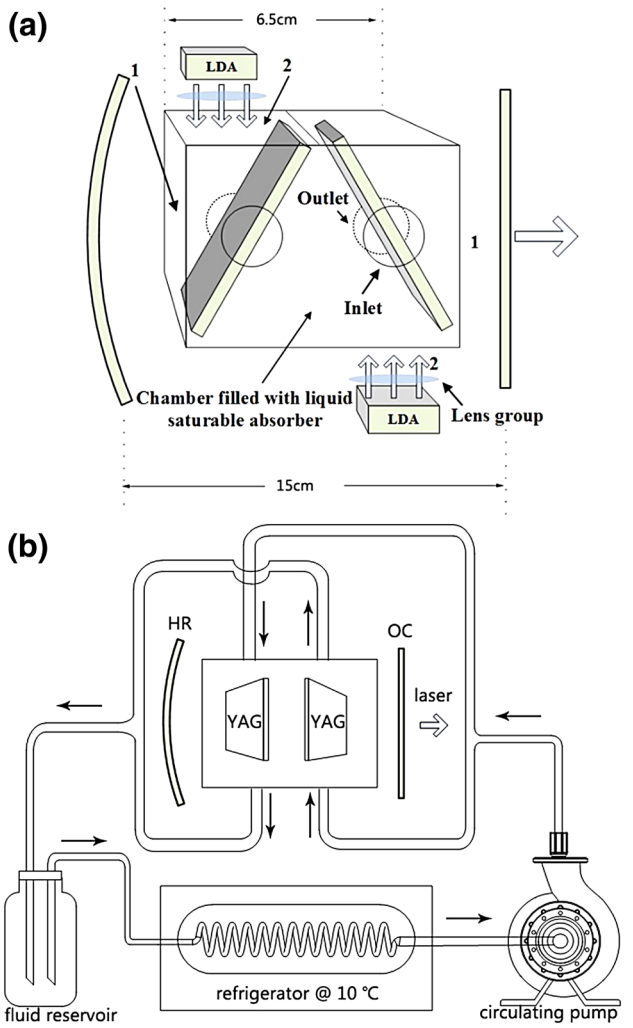

Fig. 2 Experimental setup of the Q-switched and two side liquid-cooled disk oscillator. **a** Laser oscillating and Q-switching model. **b** Circulation and liquid temperature-controlled system

of about 10×10 mm. The chamber has two kinds of windows. The first kind serves as aperture windows with antireflective coating (AR@1064 nm, relative to air), and the second kind serves as pumping windows with antireflective coating (AR@808 nm, relative to air). All windows are fused quartz. The pump beam goes through window 2 and the flowing coolant CCl_4 layer and then projects on the pump surface of the disk. The refractive index of CCl_4 matches with that of the quartz window approximately. So reflection loss at the interface between CCl_4 and quartz window is sufficiently low.

A plane output mirror (OC) and a HR mirror with a curvature radius of 500 mm were employed to make up a plano-concave resonator. The length of the cavity is 15 cm. The transmission of output mirror is different with different coolants for getting the maximum output, and the specific values are shown in part IV.

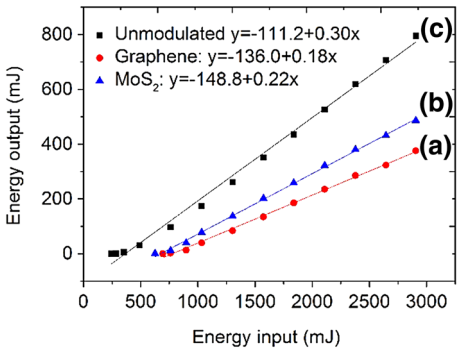

Fig. 3 Output energy versus incident pump energy. *a* Q-switched by graphene. *b* Q-switched by MoS_2. *c* Unmodulated

4 Results and discussion

Laser output is successfully obtained from the two-sided liquid cooling disk oscillator. The pump pulse width is 300 μs, and the pump repetition rate is 10 Hz. The output energy extracted from the oscillator as a function of pump energy is shown in Fig. 3. The output energy was recorded by a PE50BF high damage threshold laser probe (Ophir-Spiricon, USA) connected with the Nova II energy meter (Ophir-Spiricon, USA). The input energy is measured after the pump light being coupled by lens group.

For the unmodulated laser, the pure CCl_4 coolant and a plane output mirror of 15 % transmission were employed. By pumping with a 300-μs pulse energy of 2906 mJ at 808 nm, the maximum output energy of 795 mJ is realized corresponding to the optical–optical efficiency of 27.4 % and the slope efficiency of 30 %. The pump threshold is 243 mJ. The efficiency is not optimal because of non-uniform pumping and non-uniform flow field.

For the graphene Q-switched laser, the CCl_4 with graphene nanosheets and a plane output mirror of 40 % transmission were employed. By pumping with a 300-μs pulse energy of 2906 mJ at 808 nm, the maximum output energy of 376 mJ is realized corresponding to the optical–optical efficiency of 13 % and the slope efficiency of 18 %. The pump threshold is 694 mJ.

For the MoS_2 Q-switched laser, the CCl_4 with MoS_2 nanosheets and a plane output mirror of 30 % transmission were employed. By pumping with a 300-μs pulse energy of 2906 mJ at 808 nm, the maximum output energy of 486 mJ is realized corresponding to the optical–optical efficiency of 17 % and the slope efficiency of 22 %. The pump threshold is 626 mJ.

In Q-switched operation, the efficiency is lower than that of unmodulated laser due to the saturable loss. Furthermore, the relatively large diameter of the nanosheet brings additional scatting loss. The output energy obtained in different transmission output mirrors is listed in Table 2.

Table 2 Output energy versus different transmission output mirrors

Transmission	15 % (mJ)	20 % (mJ)	30 % (mJ)	40 % (mJ)	50 % (mJ)
Graphene	98	182	321	376	328
MoS_2	174	358	486	460	411

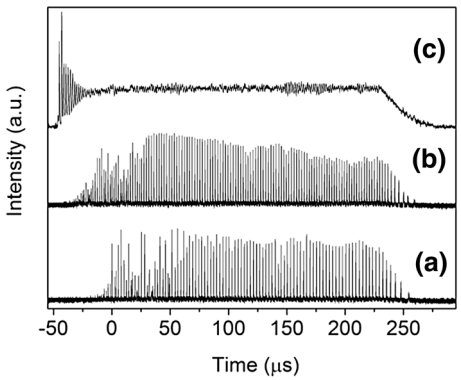

Fig. 4 Oscilloscope traces of both unmodulated and Q-switched laser. *a* Q-switched by graphene. *b* Q-switched by MoS_2. *c* Unmodulated

Three oscilloscope traces corresponding to graphene Q-switched laser output, MoS_2 Q-switched laser output, and unmodulated laser output are shown in Fig. 4; the incident pump energy is 2906 mJ. The oscilloscope trace was recorded by a DET10A/M Si-biased detector (Thorlabs, USA) and a TDS3032B oscilloscope (Tektronix, USA). In the experiment, no single Q-switched pulse was observed during one pumping process. There are two main reasons: On the one hand, non-uniform pumping, non-uniform flow field, and large nanosheet size bring high cavity loss. On the other hand, low nanosheet content means low modulation depth; as a consequence, the energy storage time is not long enough for producing a single Q-switched pulse with high energy.

The typical Q-switched pulse trains and pulse profiles are magnified in Fig. 5, the incident pump energy is 2906 mJ. For the graphene Q-switched laser, the average Q-switching repetition rate is 385 kHz and the average pulse width is 116 ns. For the MoS_2 Q-switched laser, the average Q-switching repetition rate is 470 kHz and the average pulse width is 137 ns.

Figure 6 records the evolution of the repetition rate and the pulse width with the incident pump energy. The laser output is always pulsing throughout the whole experiment. When the incident pump energy is lower than the Q-switching threshold [about 1034 mJ in (a) and 762 mJ in (b)], these pulse signals can be attributed to relaxation

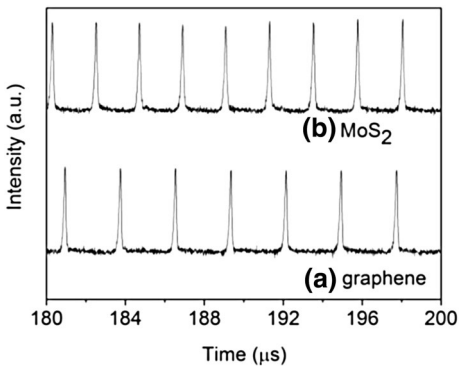

Fig. 5 Q-switched pulse trains under the incident pump energy of 2906 mJ. *a* Q-switched by graphene. *b* Q-switched by MoS2

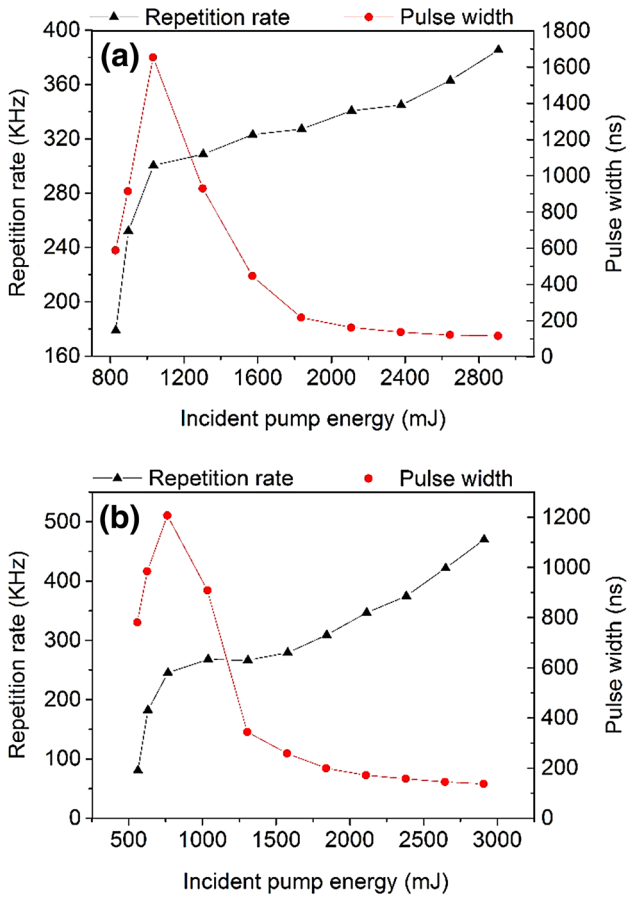

Fig. 6 Q-switched repetition rate and pulse width versus incident pump energy for Q-switched operation. **a** Graphene saturable absorber, **b** MoS_2 saturable absorber

oscillations [19]. The repetition rate and pulse width increase as the incident pump energy increases. When the incident pump energy exceeds the Q-switching threshold, the repetition rate increases and pulse width decreases as the incident pump power increases.

5 Conclusions

In this paper, a two side liquid-cooled and passively Q-switched thin-disk laser is designed by adding nanosheets into the flowing coolant. With this method, the flowing liquid can not only transfer the generated heat from the gain medium but also serve as the saturable absorber for the passively Q-switched operation. Monolayer graphene and MoS_2 nanosheets were employed in our work because they are considered to have broadband saturable absorption characteristics.

We prefer to a pump time close to the fluorescence lifetime of gain medium, so the gain medium can storage as much energy as possible. This is the best way to improve the energy of single pulse. During a pumping cycle of 300 μs, one hundred nanosecond and megahertz level Q-pulses were achieved. However, no single Q-switched pulse was observed during one pumping process. There are two main reasons: On the one hand, non-uniform pumping, non-uniform flow field, and large nanosheet size bring additional high cavity loss. On the other hand, low nanosheet content means low modulation depth; as a consequence, the energy storage time is not long enough for producing a single Q-switched pulse with high energy. Anyway, if the size of nanosheet can be decreased and the content of nanosheet in CCl_4 can be increased, the valuable single Q-switched pulse during one pumping process is promising to be obtained in this two side liquid-cooled lasers without any structural change.

The beam quality M^2 of the similar laser configuration was estimated as 50 and 10, in the vertical and horizontal direction, respectively [7]. The beam quality is so poor that it is difficult and valueless to be determined. Furthermore, the multimode laser beam in our work has a large size of 10 × 10 mm, such a large laser spot increases the difficulty in beam quality measurement. Limited to these causes, there is nearly no published experimental data on the beam quality factor of this laser configuration with large aperture. We have to say that, as shown in previous work, the beam quality of this laser configuration depends very much on the adaptive optics [20], fluid mechanics [21], and laser unstable resonator [6]. It is a complicated project, and there is a long way from outputting a laser beam with practical beam quality.

Acknowledgments This work is financially supported by the National Natural Science Foundation of China (NSFC, No. 61308086) and Natural Science Basic Research Plan in Shaanxi Province of China (No: 2016JQ6016).

References

1. S. Chénais, F. Druon, S. Forget, F. Balembois, P. Georges, Prog. Quant. Electron. **30**, 89 (2006)

2. G.F. Albrecht, S.B. Sutton, H.F. Robey, B.L. Freitas, in *Proceeding of SPIE*, ed. by G. Dube (SPIE, Los Angeles, 1989), p. 37
3. J. Vetrovec, in *Proceedings of SPIE*, ed. by C.R. Phipps (SPIE, Taos, 2002), p. 491
4. M.D. Perry, P.S. Banks, J. Zweiback, R.W. Schleicher (General Atomics), USA Patent 7366211B2, 2008
5. Mandl, D.E. Klimek, in *Conference on Lasers and Electro-Optics* (OSA, San Jose, CA, USA, 2010), p. JThH2
6. Z. Ye, Z. Cai, B. Tu, K. Wang, Q. Gao, C. Tang, C. Liu, *Proceedings of SPIE*, vol 9671 (SPIE, Beijing, China, 2015), p. 967121-1–967121-7
7. X. Fu, P. Li, Q. Liu, M. Gong, Opt. Express **22**, 18421 (2014)
8. P. Li, X. Fu, Q. Liu, M. Gong. Appl. Phys. B **119**(2), 371–380 (2015)
9. R. Nie, J. She, P. Zhao, F. Li, B. Peng, Laser Phys. Lett. **11**, 115808 (2014)
10. X.-L. Li, J.-L. Xu, Y.-Z. Wu, J.-L. He, X.-P. Hao, Opt. Express **19**, 9950 (2011)
11. Q. Wen, X. Zhang, Y. Wang, Y. Wang, H. Niu, Photon. J. IEEE **6**, 1 (2014)
12. Y.G. Wang, H.R. Chen, X.M. Wen, W.F. Hsieh, J. Tang, Nanotechnology **22**, 455203 (2011)
13. D. Mao et al., Opt. Express **23**, 27509 (2015)
14. B. Xu et al., Opt. Express **22**, 28934 (2014)
15. H. Zhang, S. Lu, J. Zheng, J. Du, S. Wen, D. Tang, K. Loh, Opt. Express **22**, 7249 (2014)
16. R.R. Nair, P. Blake, A.N. Grigorenko, K.S. Novoselov, T.J. Booth, T. Stauber, N.M. Peres, A.K. Geim, Science **320**, 1308 (2008)
17. K.F. Mak, C. Lee, J. Hone, J. Shan, T.F. Heinz, Phys. Rev. Lett. **105**, 136805 (2010)
18. A. Acrivos, A.I.Ch.E J. **6**, 584 (1960)
19. R. Dunsmuir, J. Electron. Control **10**, 453 (1961)
20. X. Fu, Q. Liu, P. Li, L. Huang, M. Gong, Opt. Express **23**, 18458 (2015)
21. P. Li, X. Fu, Q. Liu, M. Gong, J. Opt. Soc. Am. B **30**, 2161 (2013)